Supporting information.

Imidazo-pyridine-based Zinc (II) complexes as fluorescent hydrogen sulfide probes.

Maria Strianese*[a], Stefano Brenna, G. Attilio Ardizzoia, Daniela Guarnieri [a], Marina Lamberti [a], Ilaria D'Auria [a], Claudio Pellecchia [a].

[a]Dipartimento di Chimica e Biologia "Adolfo Zambelli", Università degli Studi di Salerno, Via Giovanni Paolo II, 132, 84084 Fisciano (SA) Italy; [b]Dipartimento di Scienza e Alta tecnologia, Università dell'Insubria and CIRCC, via Valleggio, 9, 22100 Como, Italy.

Contents

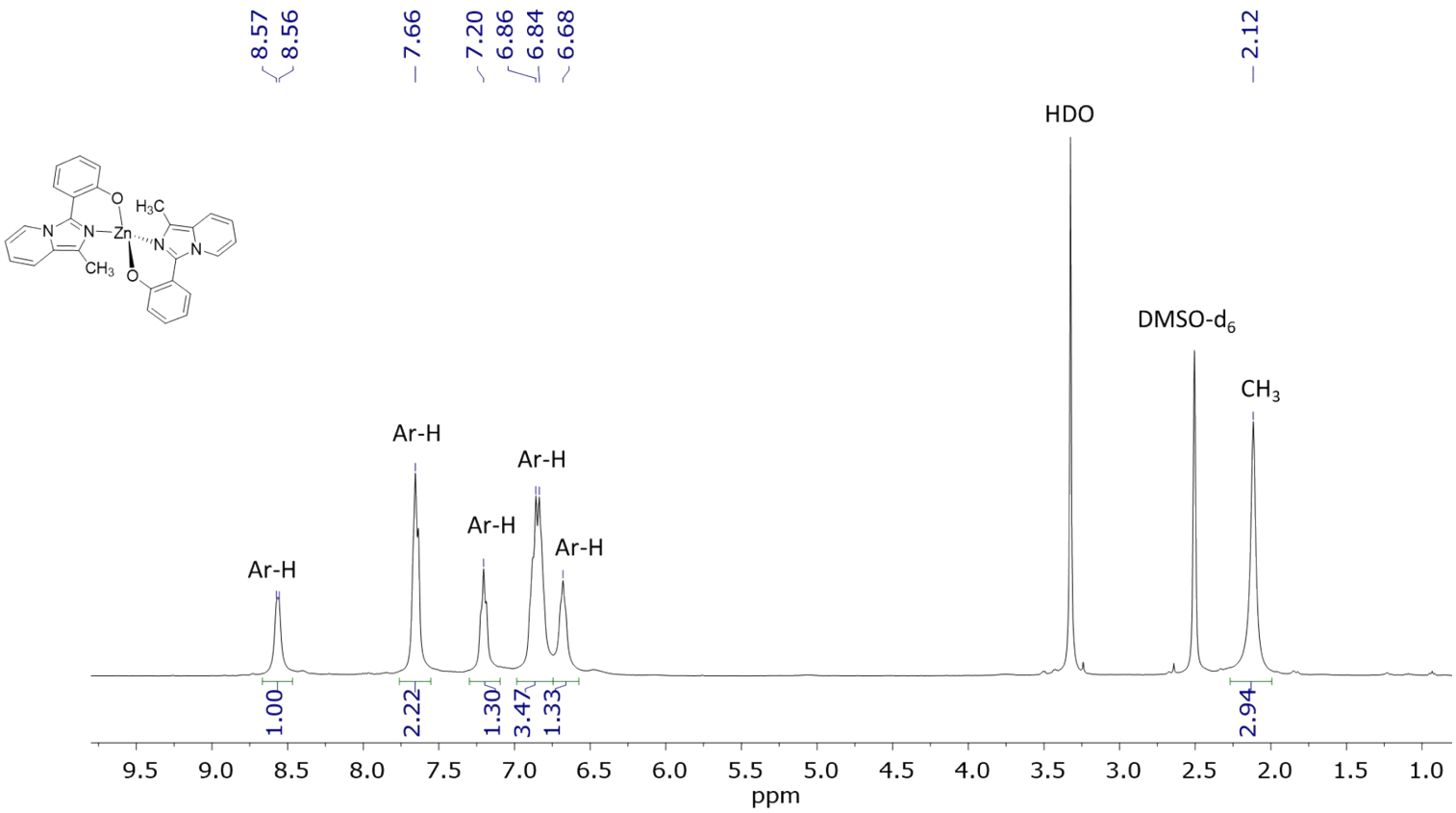

Figure S1. ^{1}H NMR spectrum of complex **1** in DMSO-d_6. [complex **1**] = $1.9 \cdot 10^{-2}$ M.

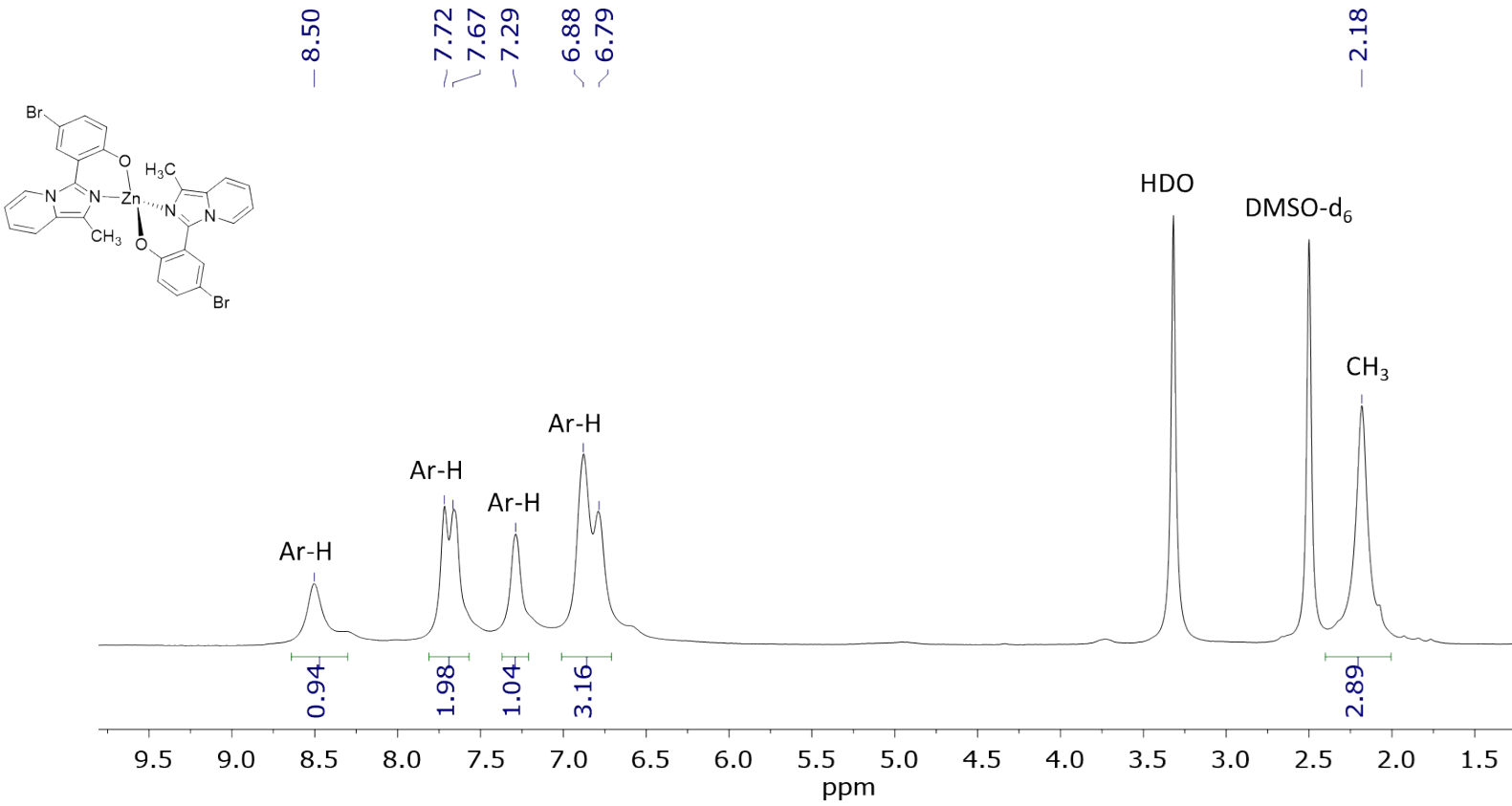

Figure S2. ^{1}H NMR spectrum of complex **2** in DMSO-d_6. [complex **2**] = $1.5 \cdot 10^{-2}$ M.

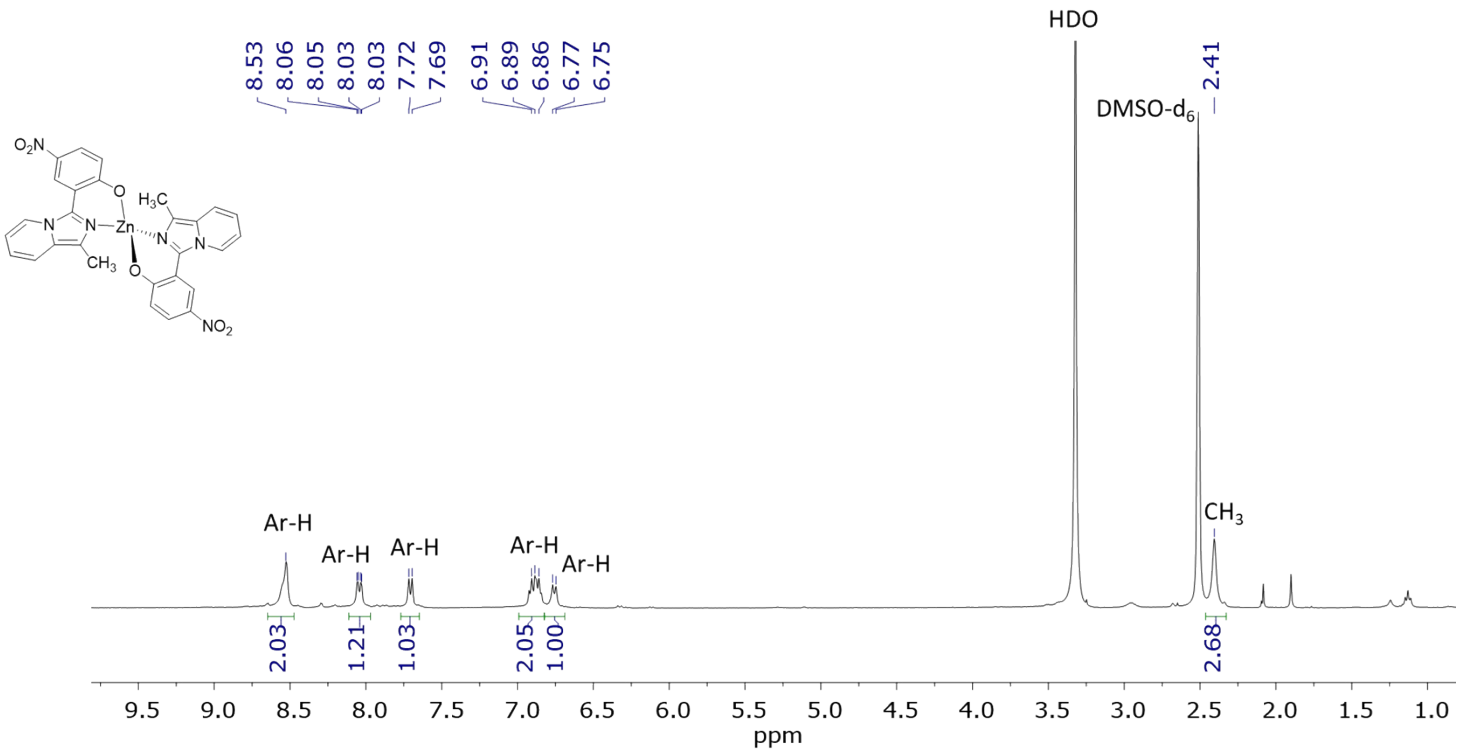

Figure S3. ^{1}H NMR spectrum of complex **3** in DMSO-d_6. [complex **3**] = $1.7 \cdot 10^{-2}$ M.

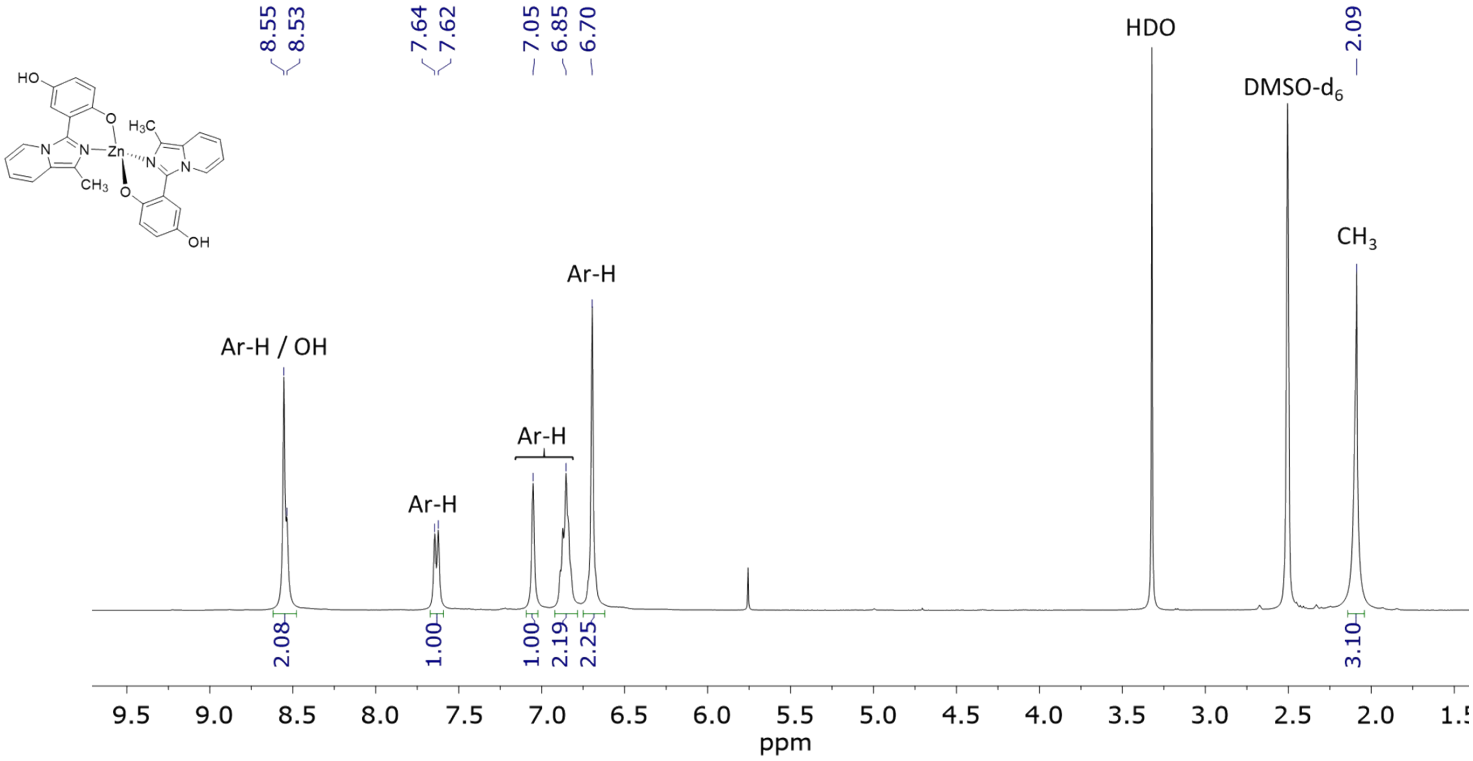

Figure S4. ^{1}H NMR spectrum of complex **4** in DMSO-d_6. [complex **4**] = $1.8 \cdot 10^{-2}$ M.

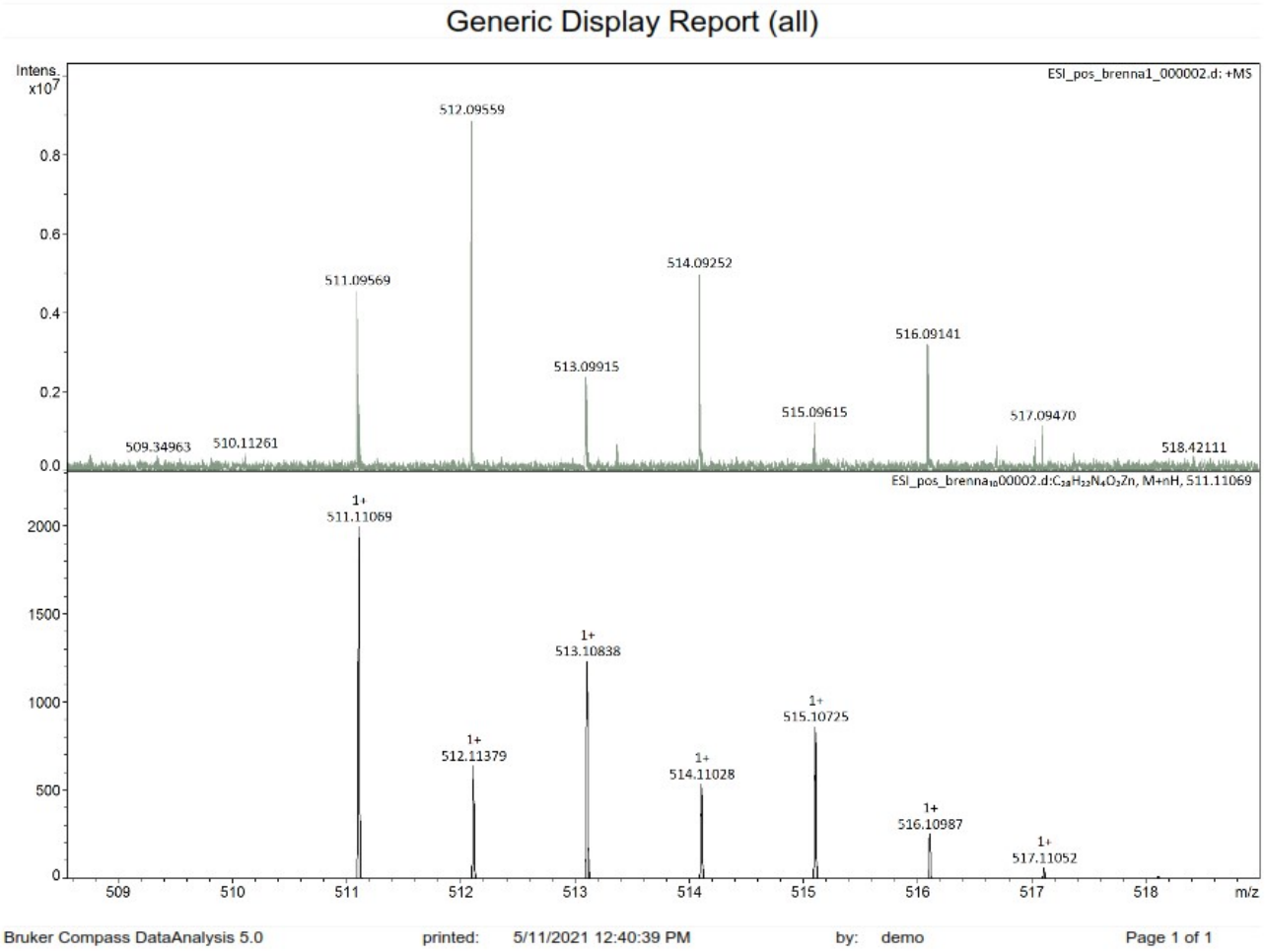

Figure S5. Enlargement of the ESI spectrum of complex **1** in THF. The upper trace is the experimental trace whereas the lowers are the theoretical ones.

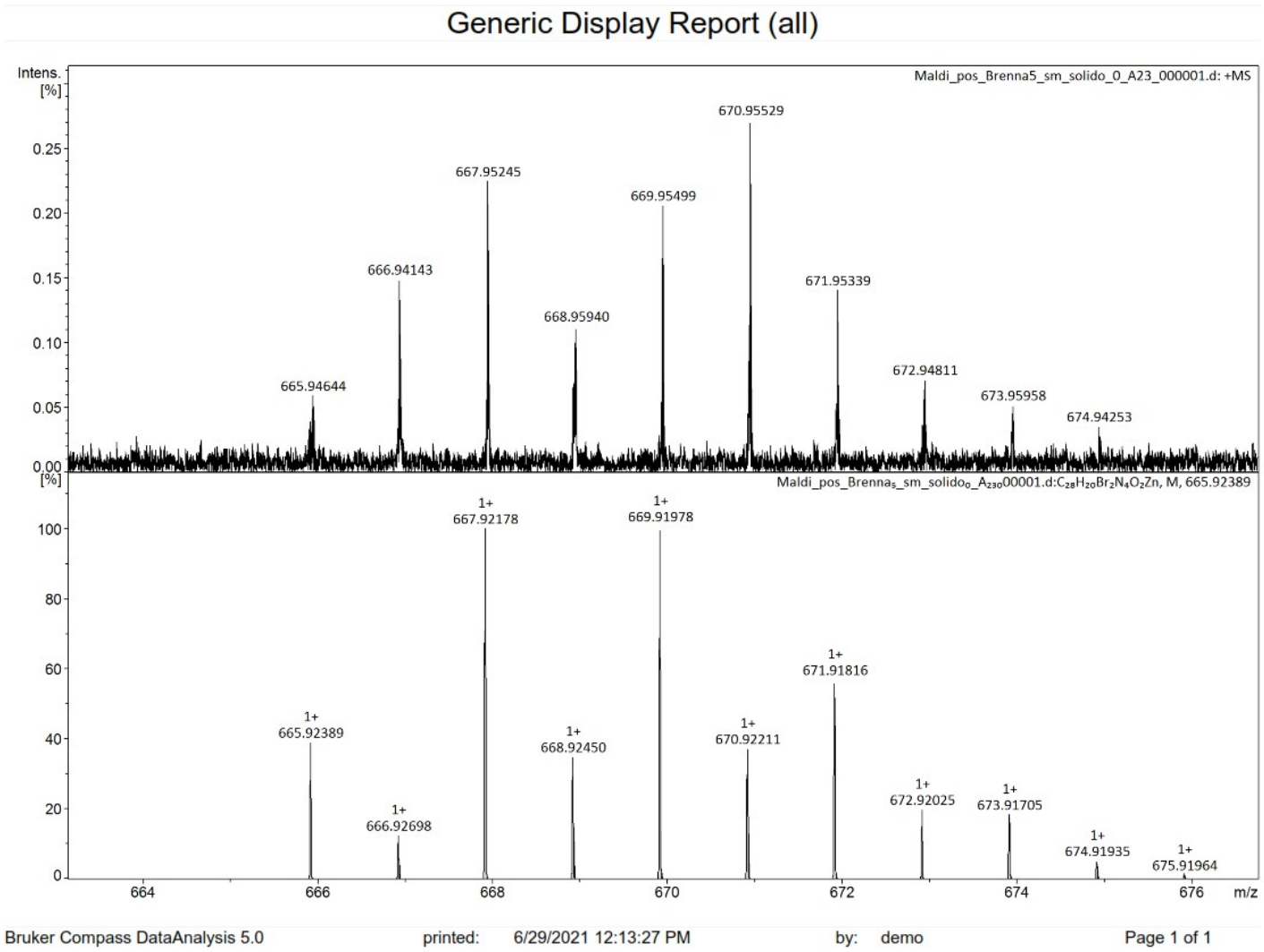

Figure S6. Enlargement of the MALDI spectrum of complex **2**. The upper trace is the experimental trace whereas the lowers are the theoretical ones.

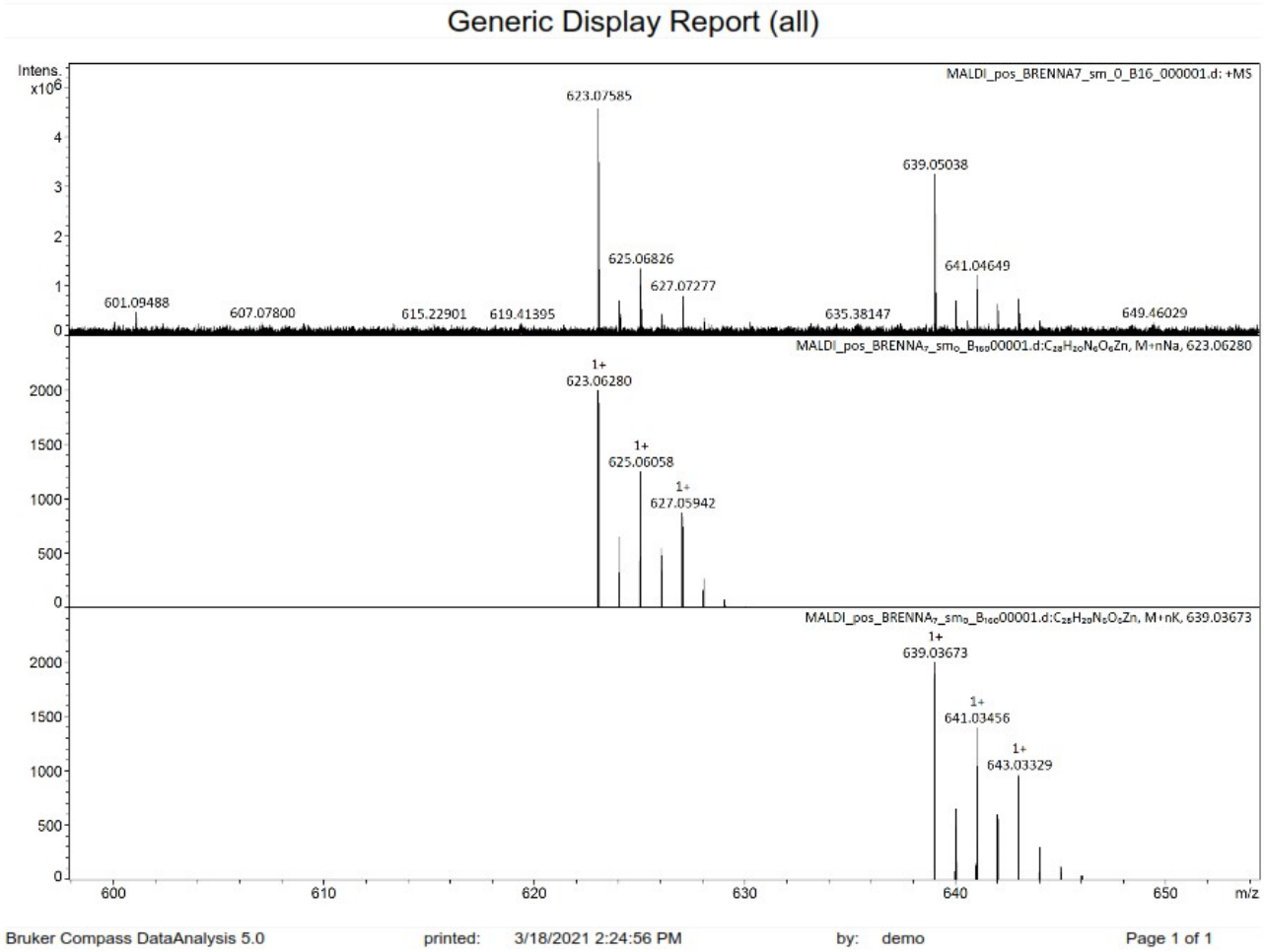

Figure S7. MALDI spectrum of complex **3** in MeOH. The upper trace is the experimental trace whereas the lowers are the theoretical ones.

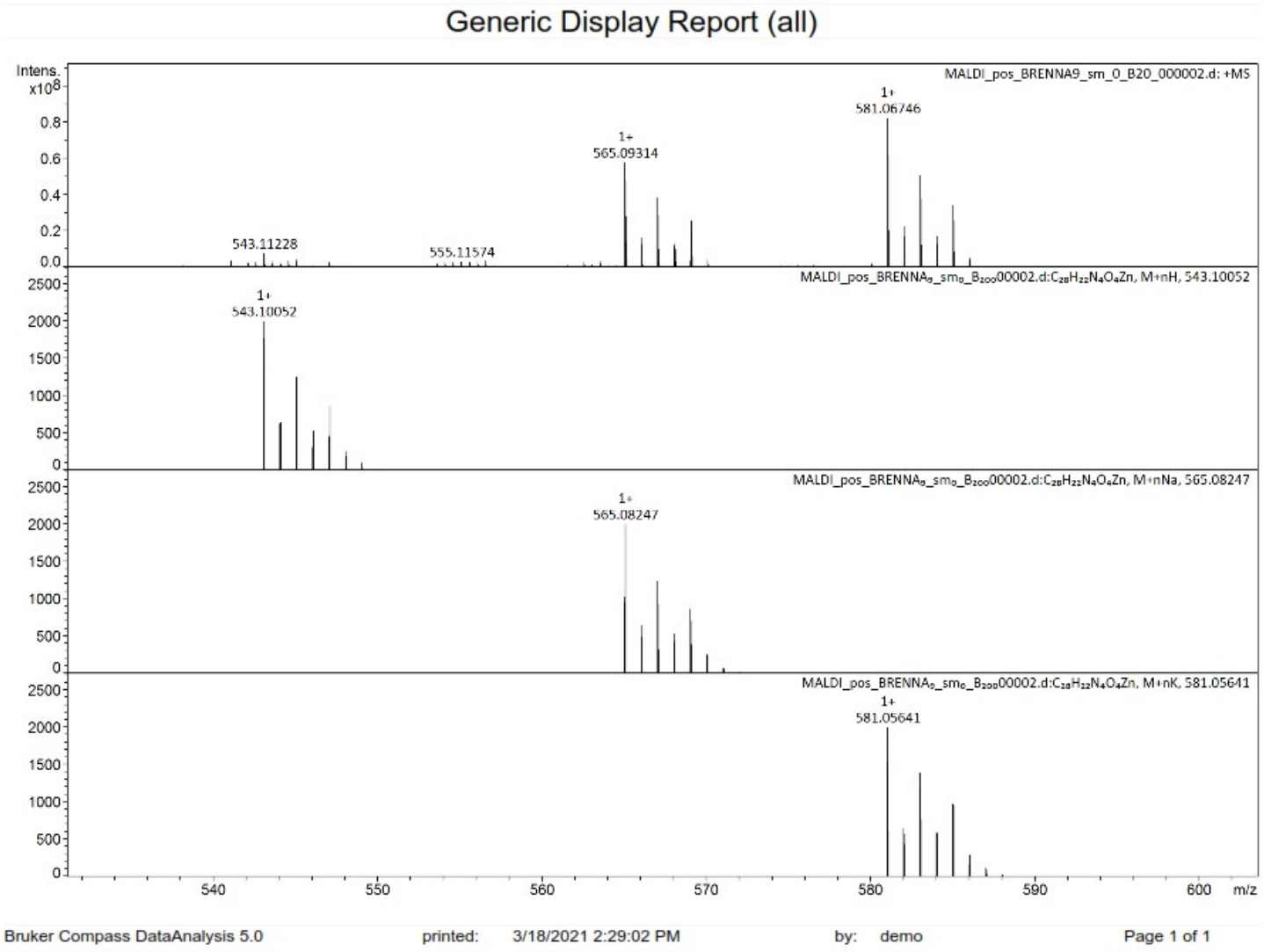

Figure S8. MALDI spectrum of complex **4** in MeOH. The upper trace is the experimental trace whereas the lowers are the theoretical ones.

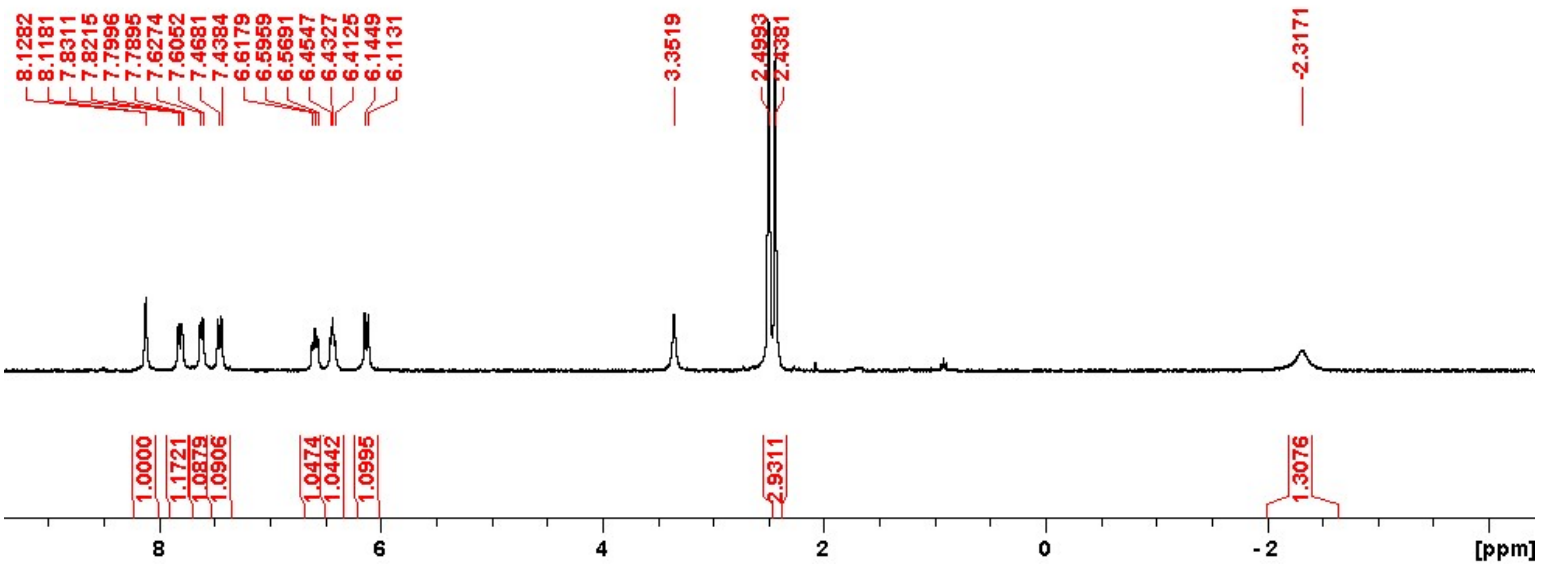

Figure S9. ^{1}H NMR spectrum of complex **3** in DMSO-d_6 after the addition of an excess of HS^{-}.

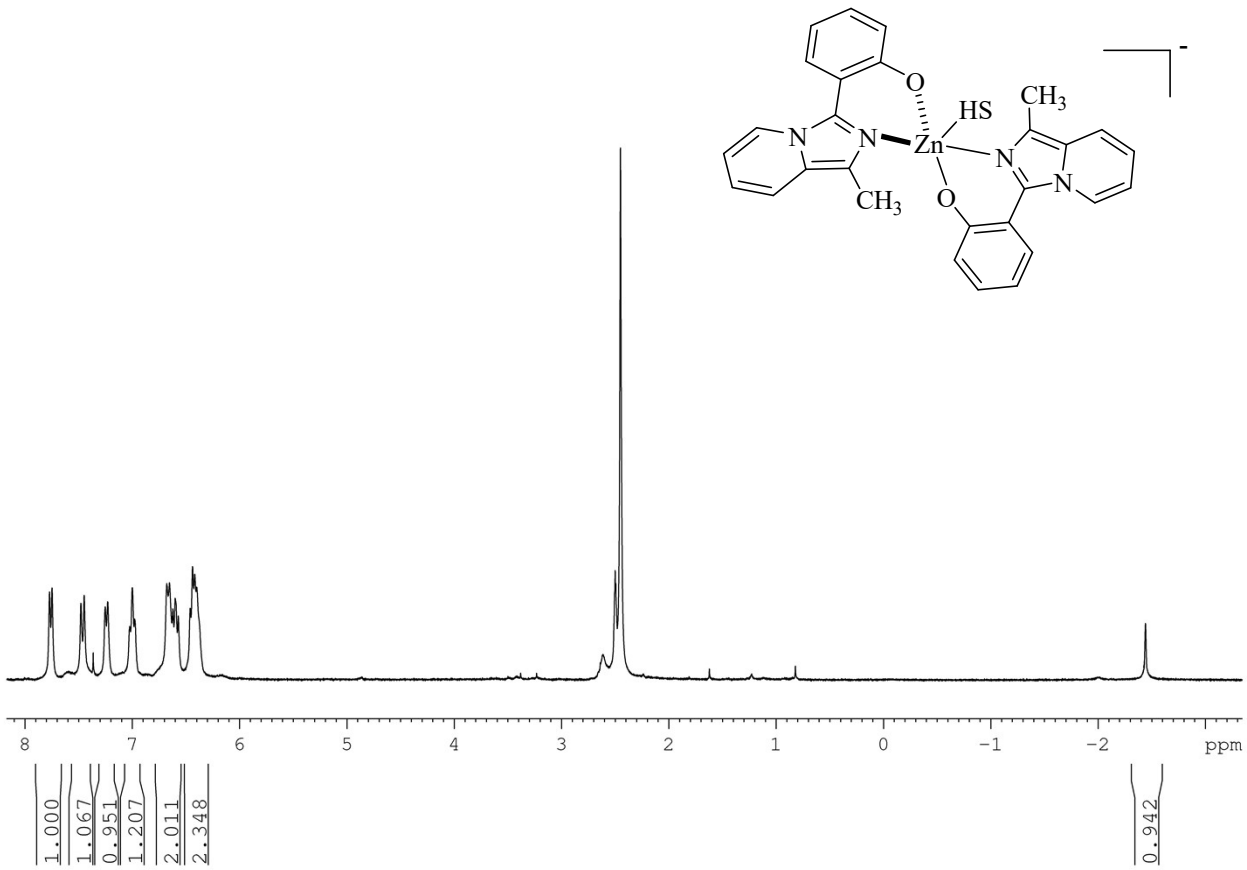

Figure S10. ^{1}H NMR spectrum of complex **1** in DMSO-d_6 after the addition of an excess of HS^{-}.

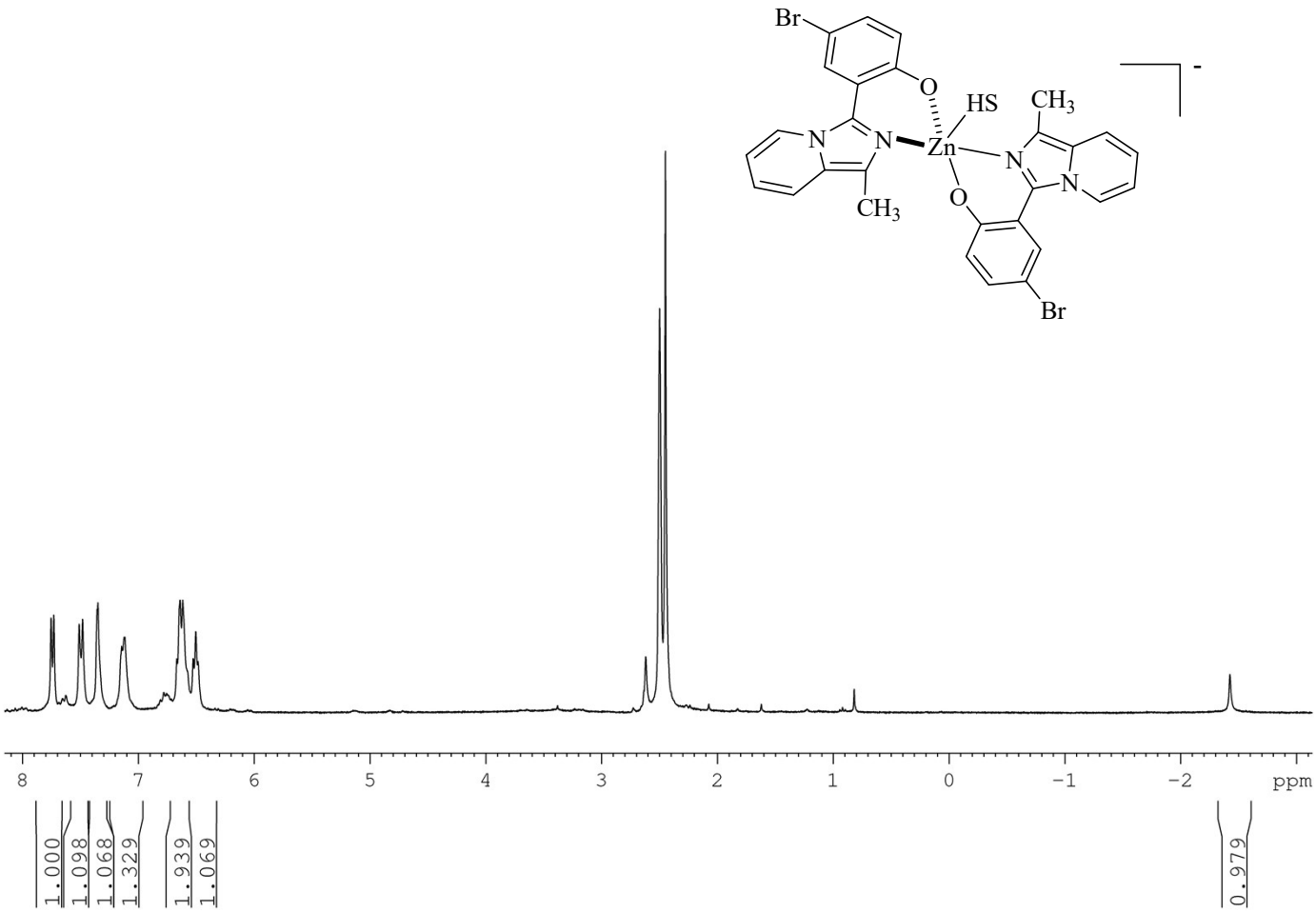

Figure S11. ^{1}H NMR spectrum of complex **2** in DMSO-d_6 after the addition of an excess of HS^{-}.

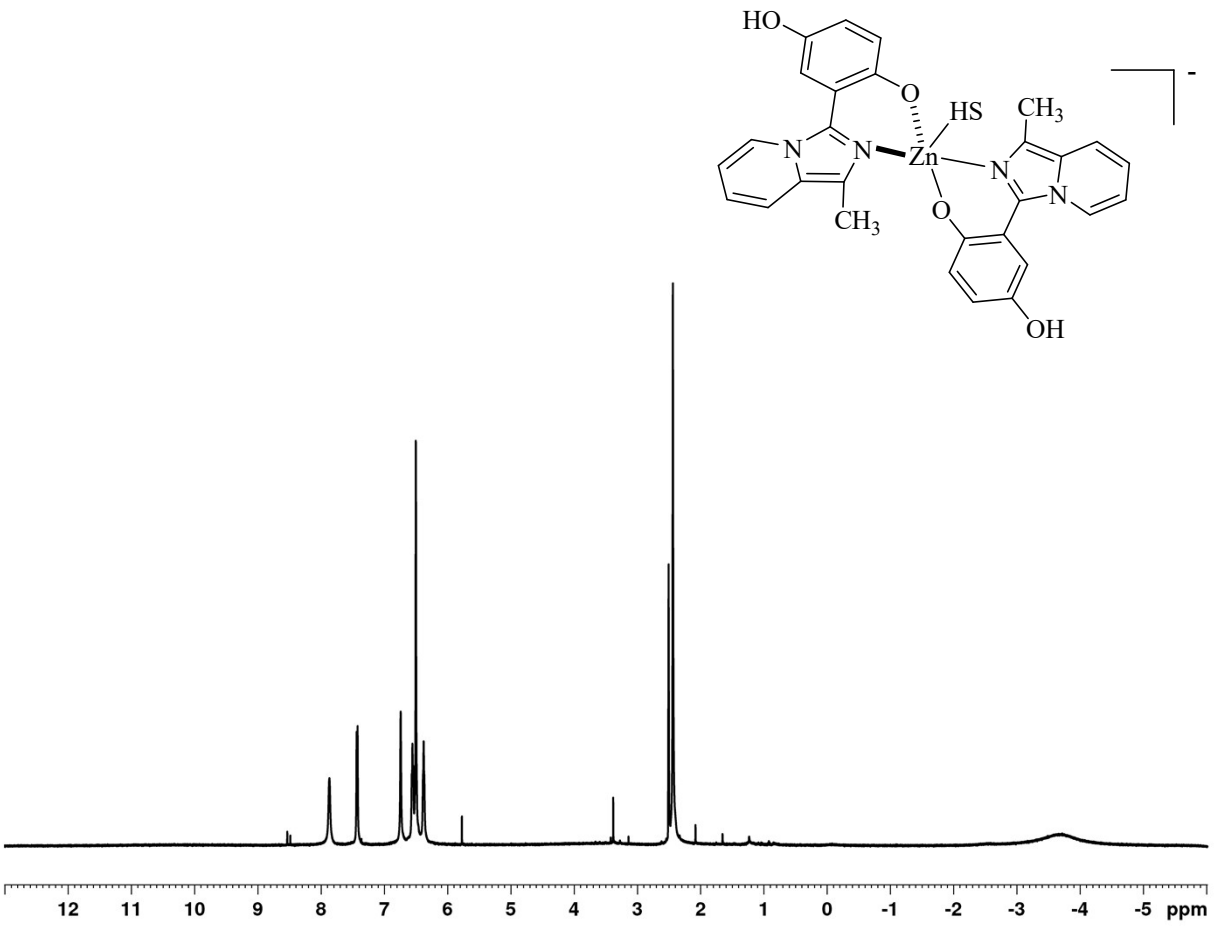

Figure S12. ^{1}H NMR spectrum of complex **4** in DMSO-d_6 after the addition of an excess of HS^{-}.

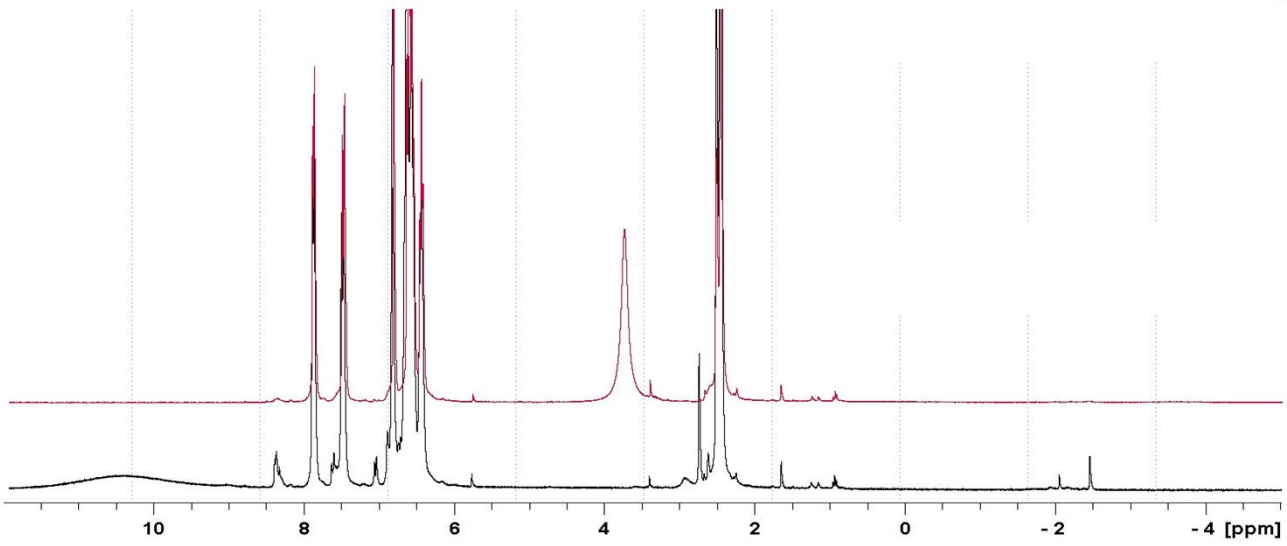

Figure S13. ^{1}H NMR spectrum of complex **4** in dried DMSO-d_6 after the addition of an excess of HS^- (black trace), and after the subsequent addtion of 10 μL of D_2O (red trace).

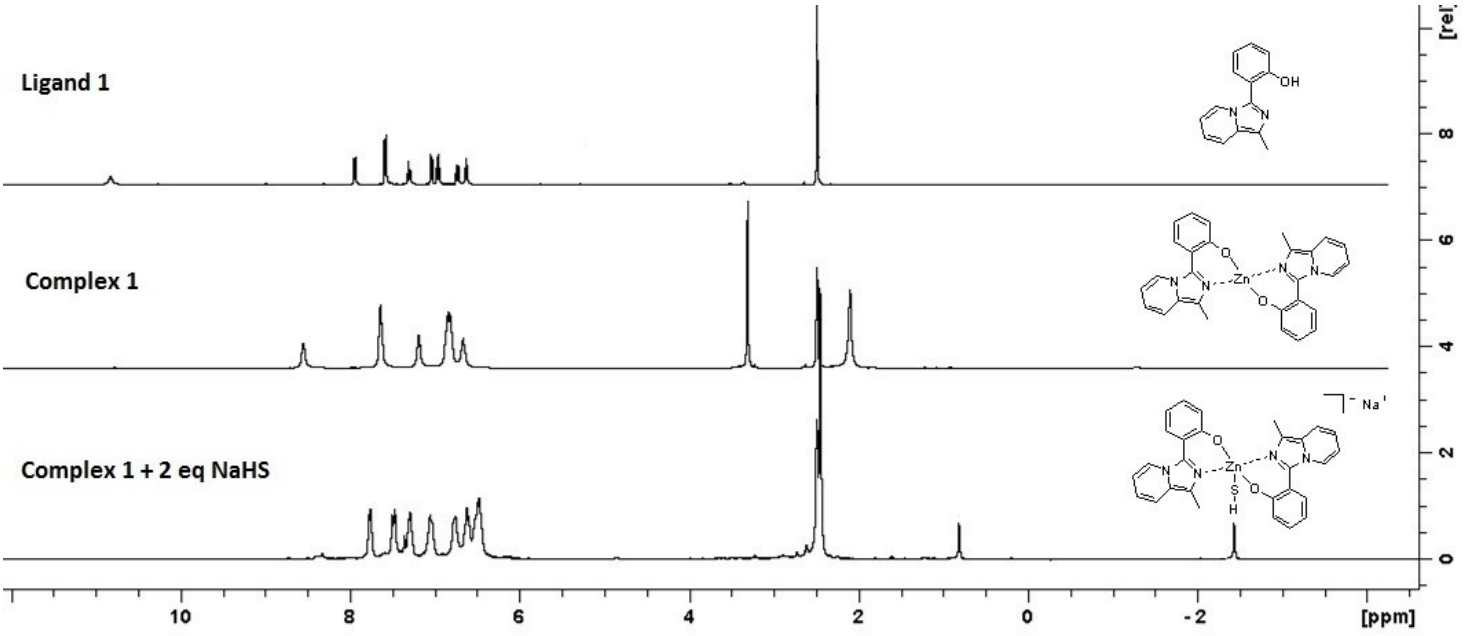

Figure S14. ^{1}H NMR spectra of complex **1** in DMSO-d_6 after the addition of an excess of HS^- (lower trace), of complex **1** free (middle trace) of ligand **1** (upper trace). [complex **1**] = 5×10^{-2} M; [NaSH] = 0.1 M.

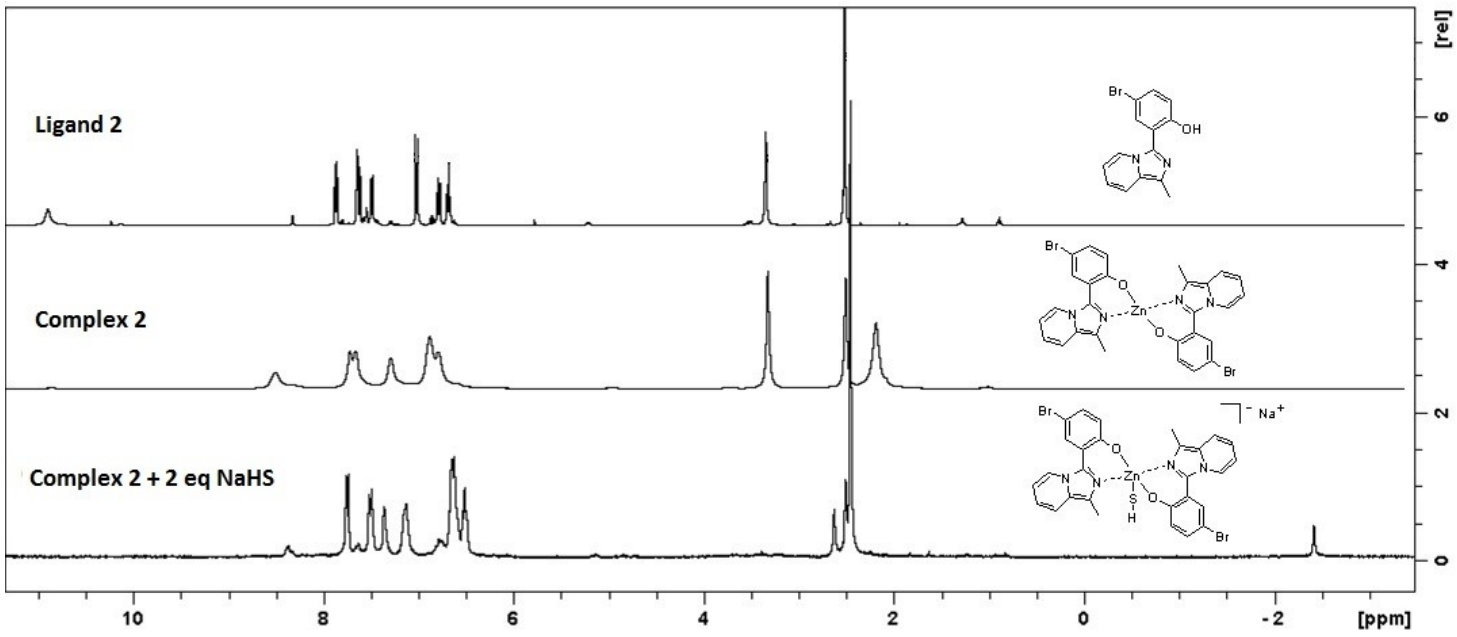

Figure S15. ^{1}H NMR spectra of complex **2** in DMSO-d_6 after the addition of an excess of HS^- (lower trace), of complex **2** free (middle trace) of ligand **2** (upper trace). [complex **2**] = 5×10^{-2} M; [NaSH] = 0.1 M.

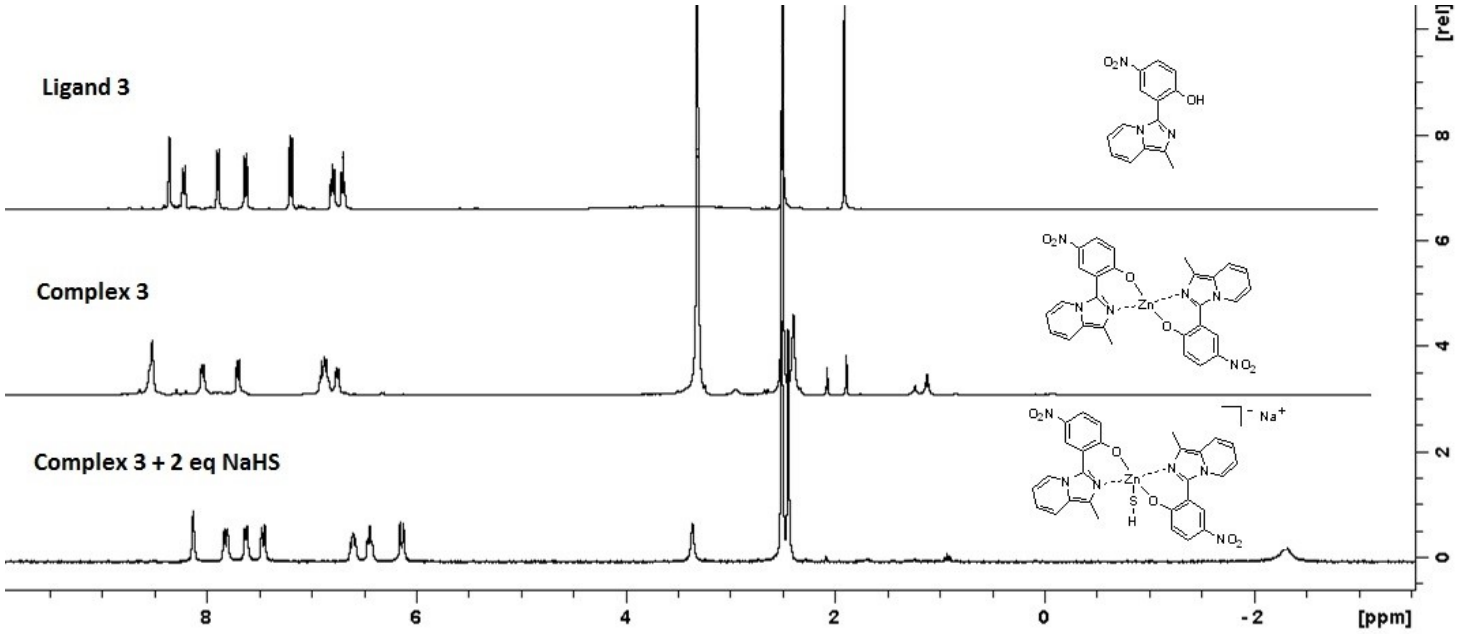

Figure S16. ^{1}H NMR spectra of complex **3** in DMSO-d_6 after the addition of an excess of HS^- (lower trace), of complex **3** free (middle trace) of ligand **3** (upper trace). [complex **3**] = 5×10^{-2} M; [NaSH] = 0.1 M.

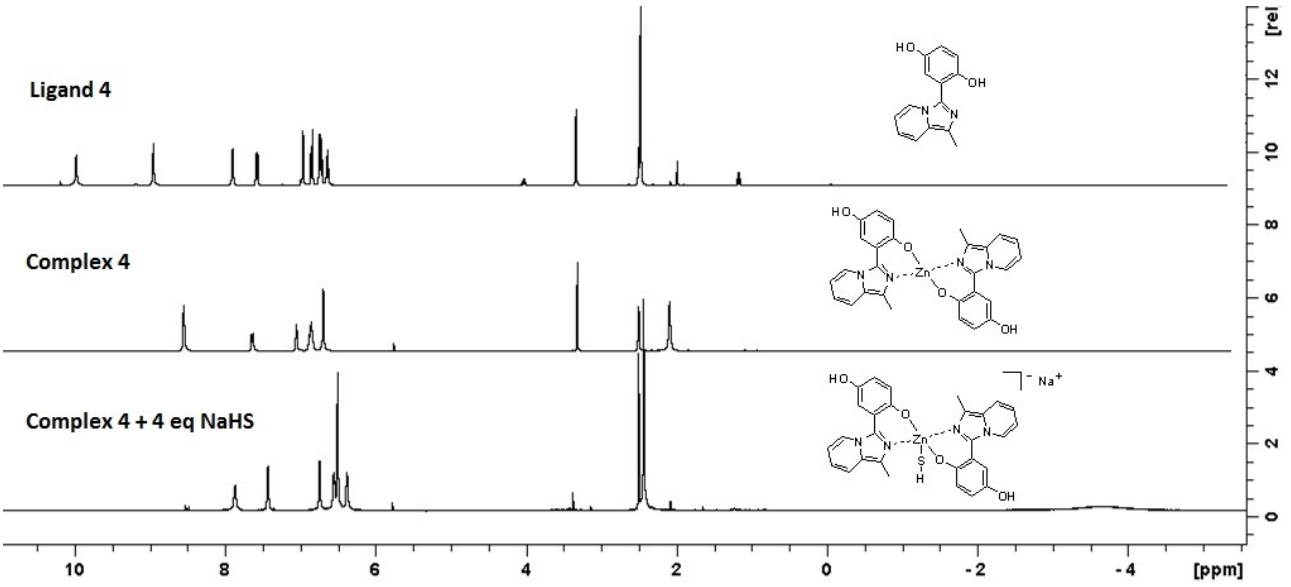

Figure S17. ^{1}H NMR spectra of complex **4** in DMSO-d_6 after the addition of an excess of HS^- (lower trace), of complex **4** free (middle trace) of ligand **4** (upper trace). [complex **4**] = 5×10^{-2} M; [NaSH] = 0.1 M.

	HOMO	LUMO		HOMO	LUMO
1	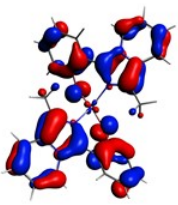	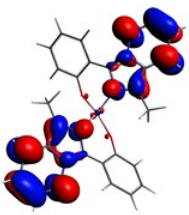	**1** + HS^-	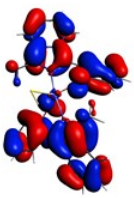	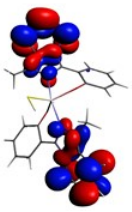
2	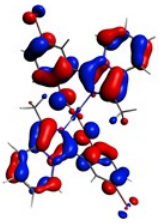	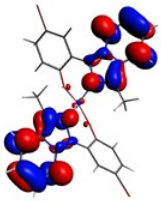	**2** + HS^-	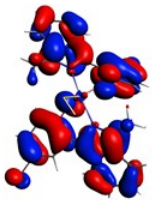	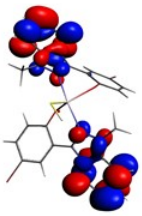
3	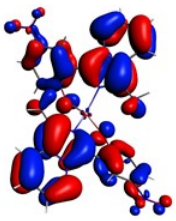	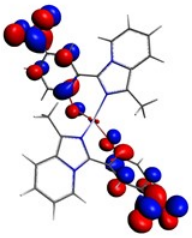	**3** + HS^-	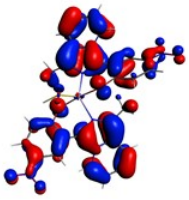	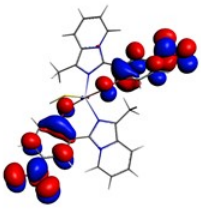
4	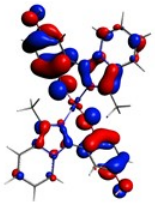	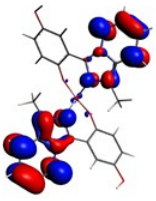	**4** + HS^-	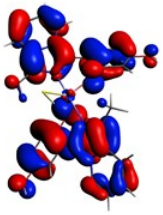	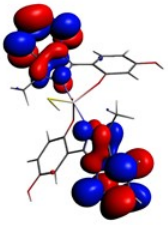

Figure S18. HOMO and LUMO orbitals calculated for complexes **1**-**4** and their adducts with HS-.

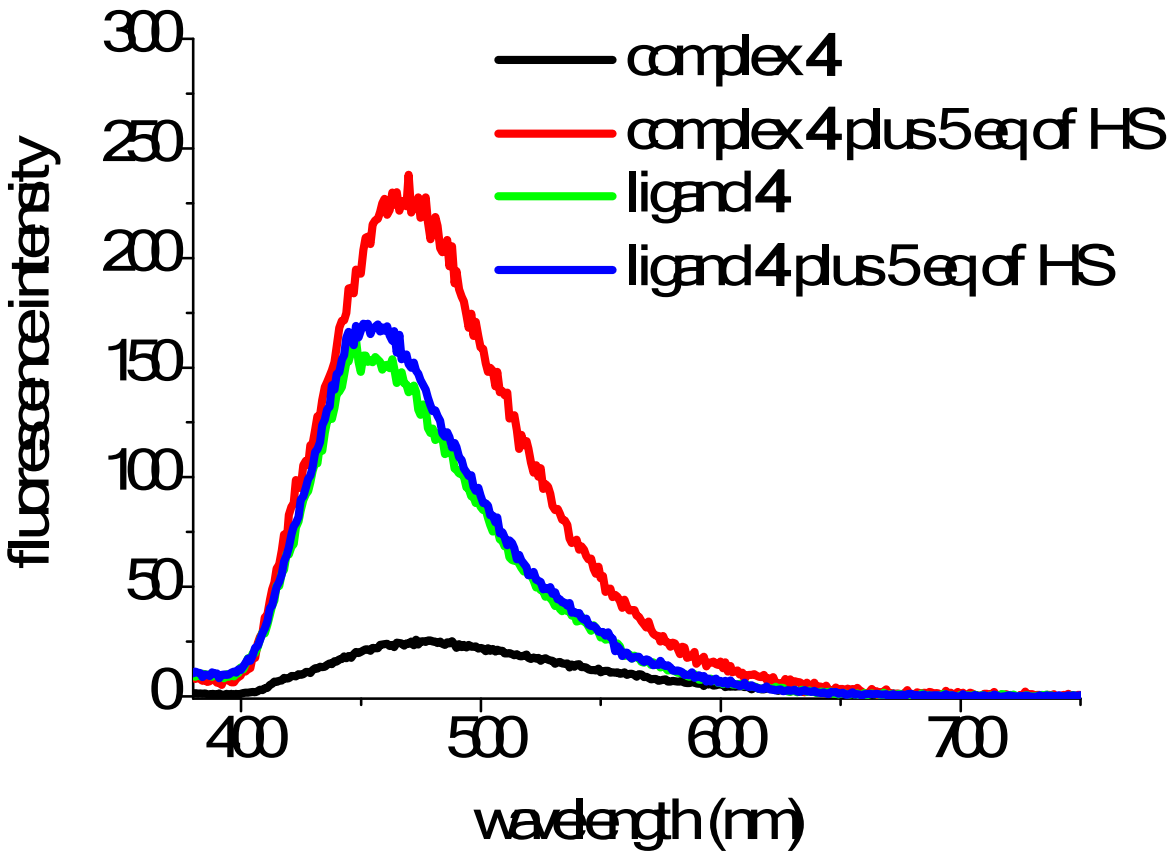

Figure S19. Emission spectra of complex **4** and of ligand **4** before and after the addition of 5 equiv of NaSH. [Complex **4**] = 1×10^{-5} M; [ligand **4**] = 1×10^{-5} M; [NaSH] = 5×10^{-5} M. All spectra were measured in DMSO with λ_{exc} = 370 nm for complex **4** and λ_{exc} = 340 nm for ligand **4**.

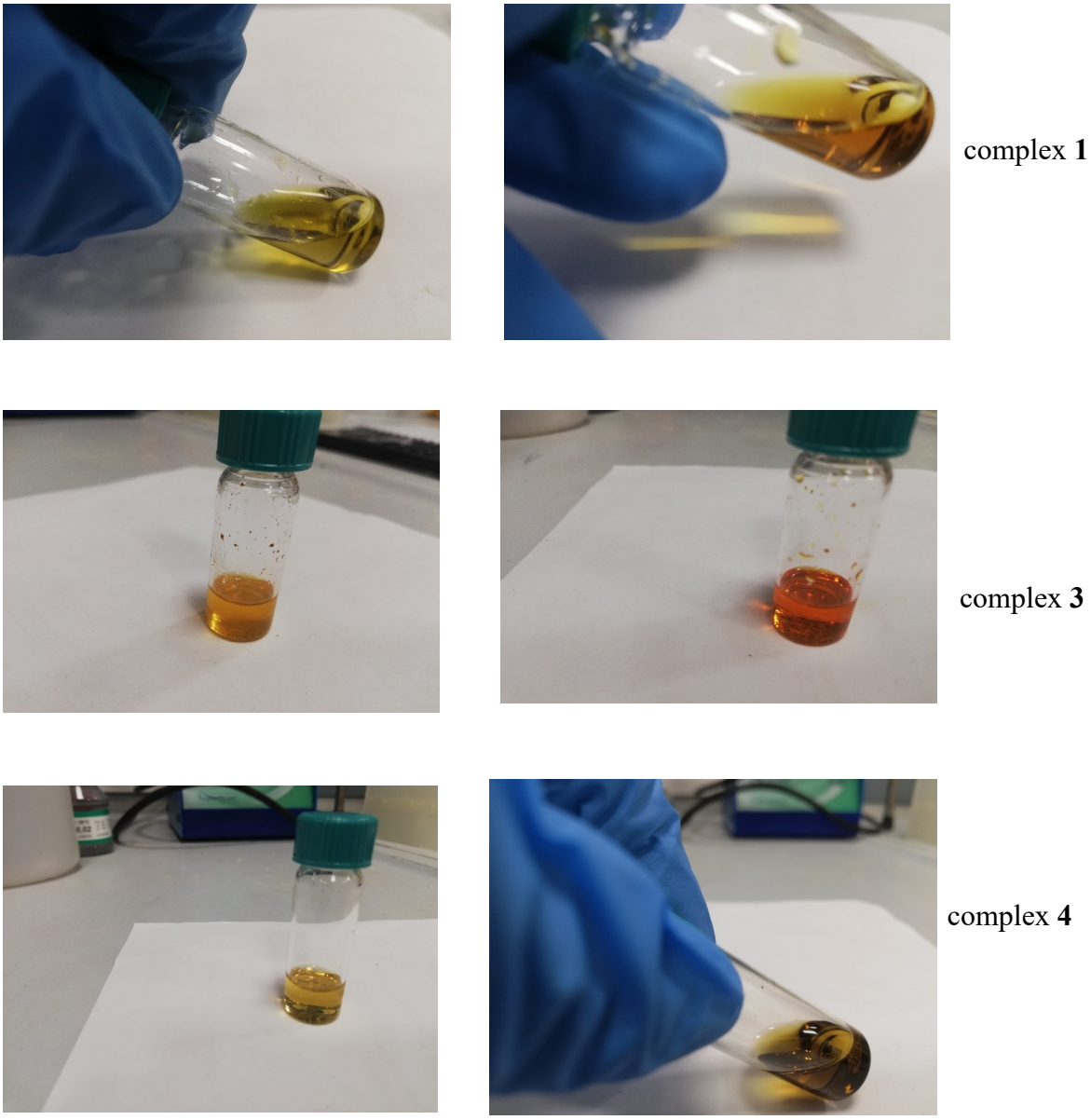

Figure S20. Real color images of DMSO solutions of complexes **1**, **3** and **4** before (left column) and after treatment with 5 equivs of HS^- (right column).

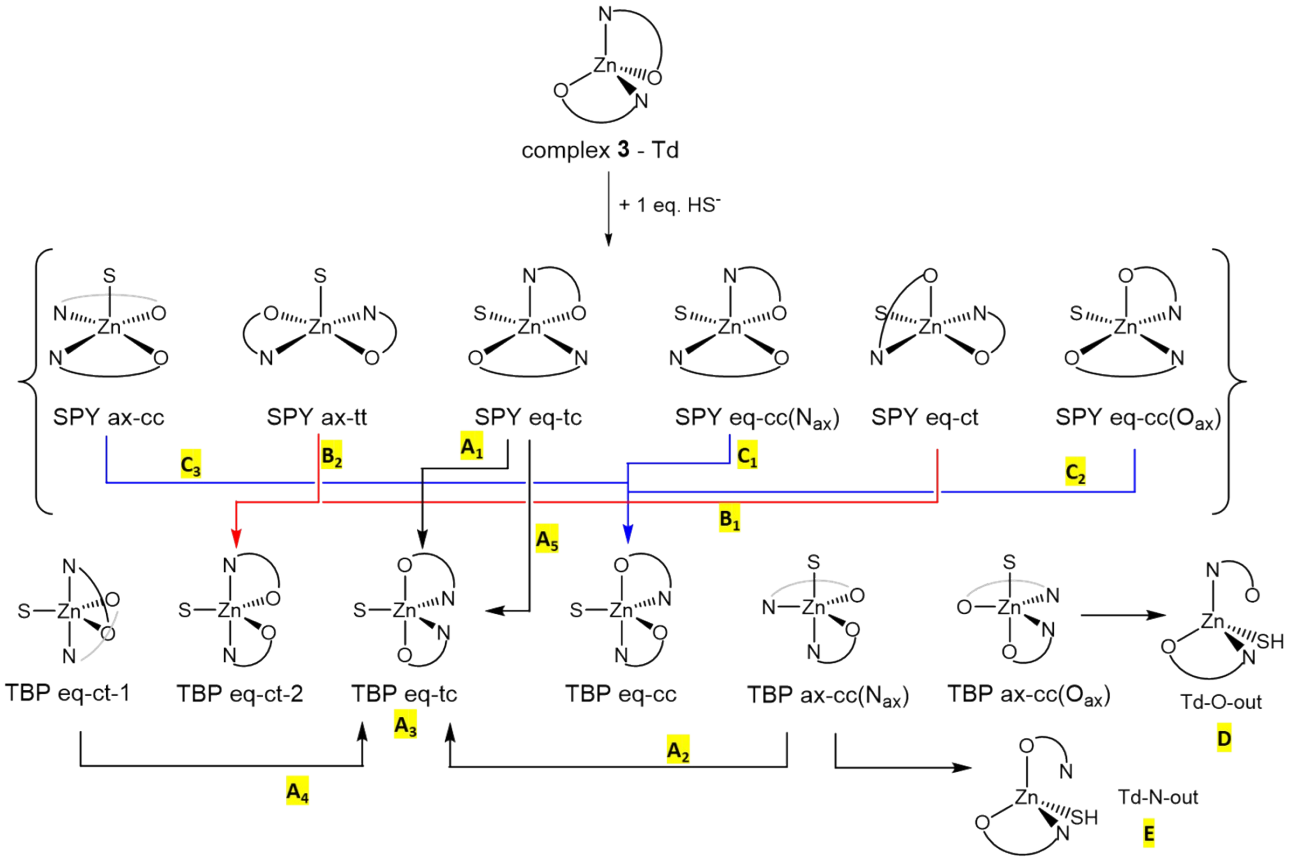

Figure S21. Possible SPY and TBP structures resulting from the reaction of complex **3** (Td) with one equivalent of HS^-. The different isomers are indicated by capital letters (**A**-**E**). Subscripts refer to different optimization processes leading to the same isomer ($\mathbf{A_1}$-$\mathbf{A_5}$). See main text for notation.

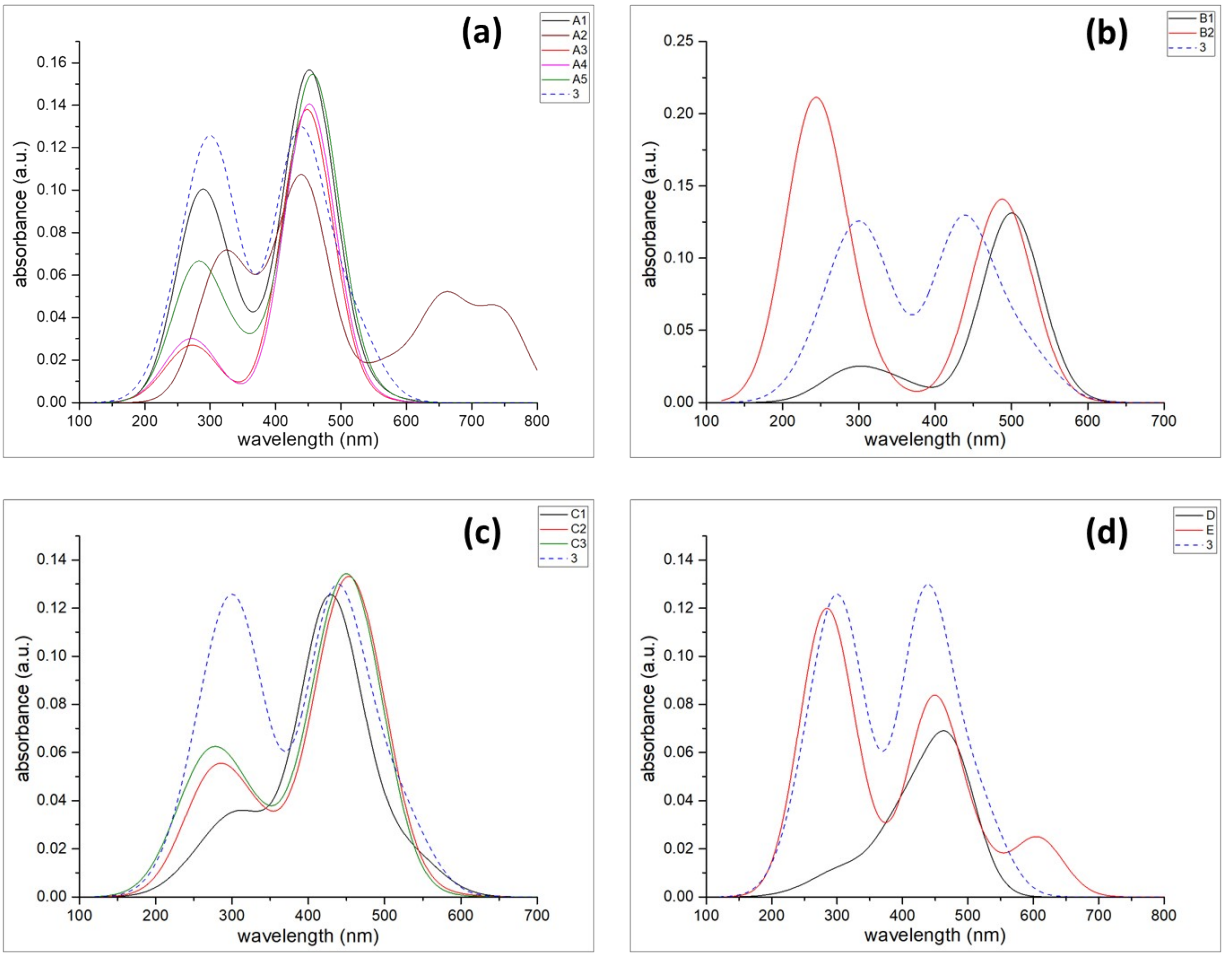

Figure S22. UV-vis spectra in DMSO solution calculated for structures **A** (a), **B** (b), **C** (c) and **D**,**E** (d), compared with the experimental trace recorded for complex **3** (dashed blue line). Structure $\mathbf{A_1}$ (black trace in (a)) shows the better fit with the experimental UV.

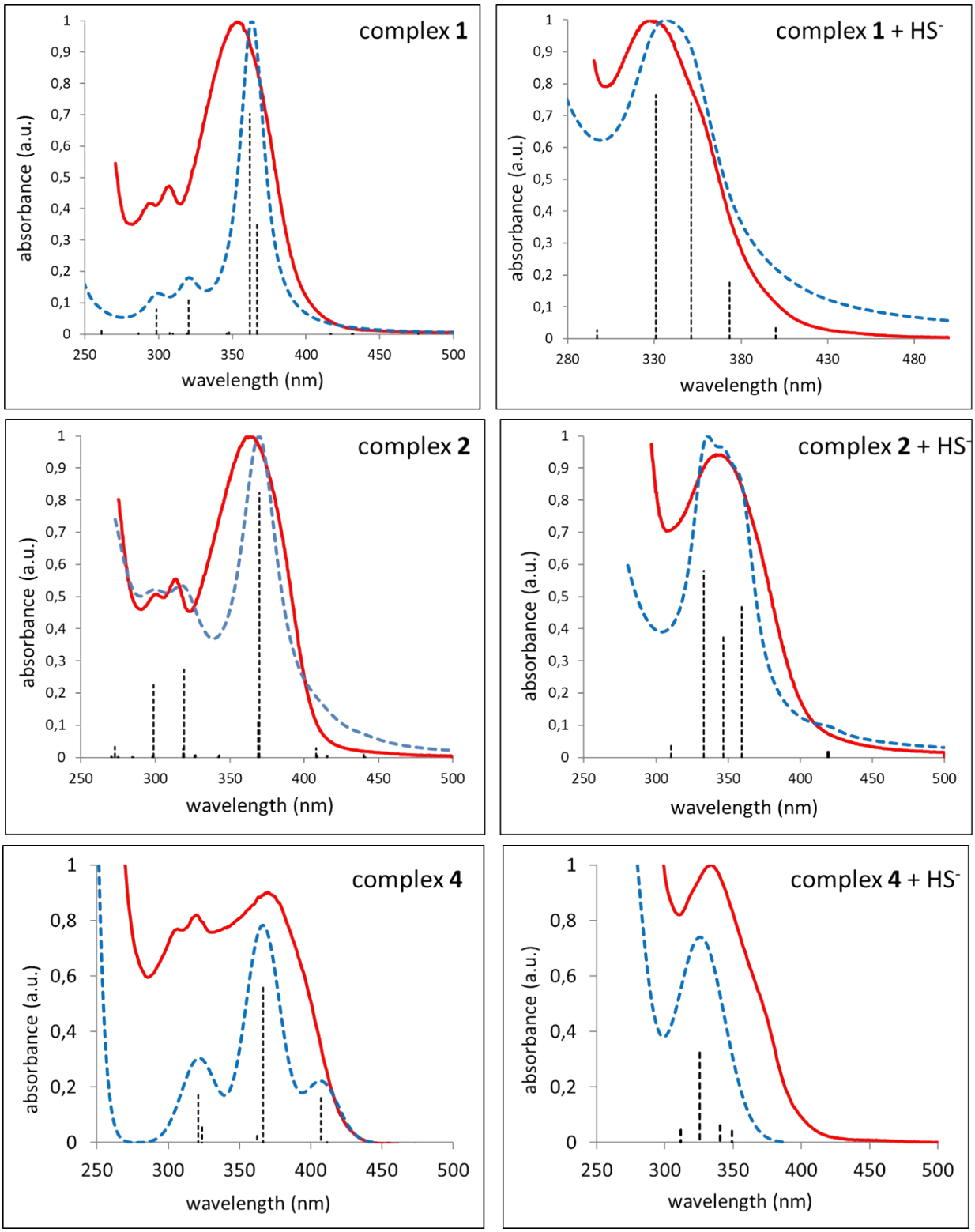

Figure S23. Normalized calculated (dashed blue) and experimental (red line) UV-vis spectra in DMSO solution for complexes **1**, **2** and **4** and their adducts with HS^-. Dashed black bars represent vertical transitions with oscillator strength $f > 0.01$

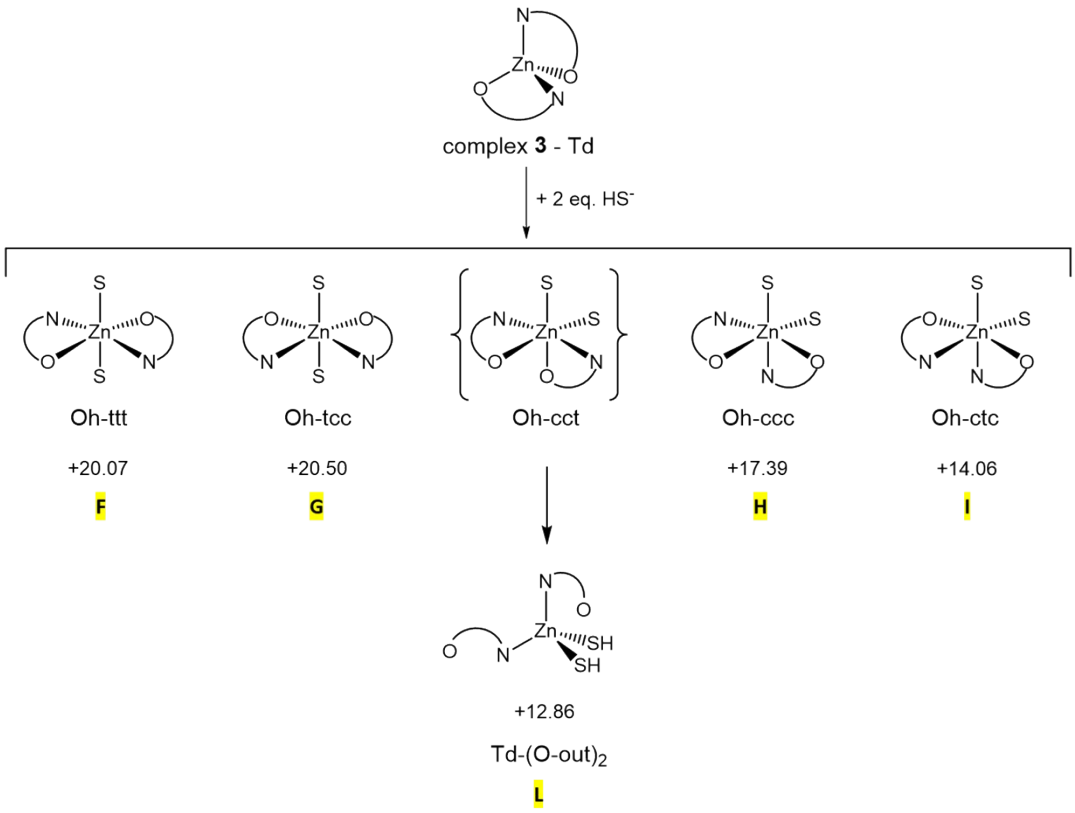

Figure S24. Possible octahedral structures resulting from the reaction of complex **3** (Td) with two equivalents of HS^-. Numbers represent the computed ΔG values for each optimization process.

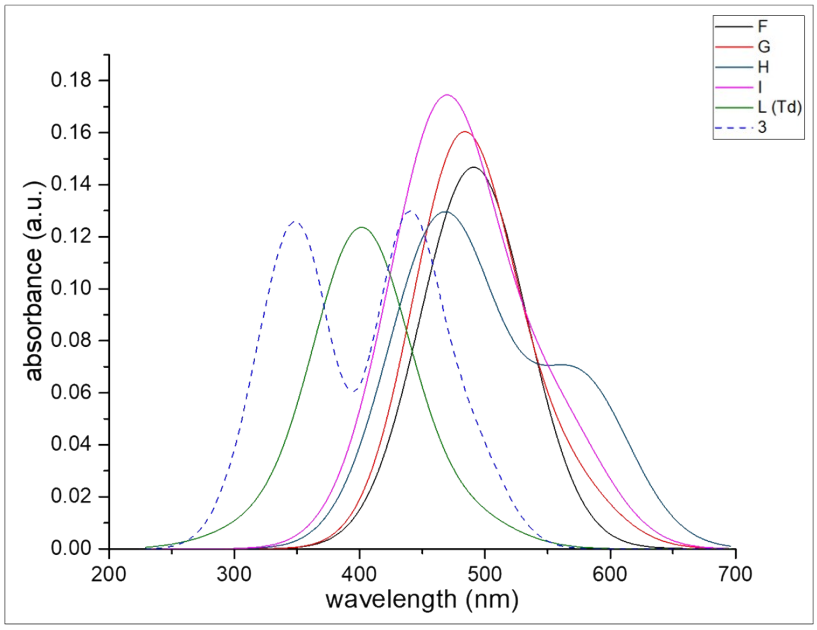

Figure S25. Calculated UV-vis spectra in DMSO solution for octahedral structures **F**-**I** and for tetrahedral structure **L**, compared with the experimental trace recorded for complex **3** (dashed blue line).